


## Article

# Colorimetric Chemosensor Based on Fe<sub>3</sub>O<sub>4</sub> Magnetic Molecularly Imprinted Nanoparticles for Highly Selective and Sensitive Detection of Norfloxacin in Milk

Maiquan Li , Lingli Luo, Jiayin Li, Yingzi Xiong, Ling Wang and Xia Liu \*

Hunan Provincial Key Laboratory of Food Science and Biotechnology, College of Food Science and Technology, Hunan Agricultural University, Changsha 410128, China

\* Correspondence: liuxiaspr@aliyun.com; Tel.: +86-731-84673517

**Abstract:** Long-term use of norfloxacin (NOR) will cause NOR residues in foods and harm human bodies. The determination of NOR residues is important for guaranteeing food safety. In this study, a simple, selective, and label-free colorimetric chemosensor for in situ NOR detection was developed based on Fe<sub>3</sub>O<sub>4</sub> magnetic molecularly imprinted nanoparticles (Fe<sub>3</sub>O<sub>4</sub> MMIP NPs). The Fe<sub>3</sub>O<sub>4</sub> MMIP NPs showed good peroxidase-like catalytic activity to 3,3',5,5'-tetramethylbenzidine (TMB) and selective adsorption ability to NOR. The colorimetric chemosensor was constructed based on the Fe<sub>3</sub>O<sub>4</sub> MMIP NPs-H<sub>2</sub>O<sub>2</sub>-TMB reaction system. The absorbance differences were proportional to the concentrations of NOR in the range of 10–300 ng/mL with a limit of detection at 9 ng/mL. The colorimetric chemosensor was successfully applied to detect NOR residue in milk. The recovery range was 78.2–95.81%, with a relative standard deviation of 2.1–9.88%. Together, the proposed colorimetric chemosensor provides a reliable strategy for the detection of NOR residues in foods.

**Keywords:** Fe<sub>3</sub>O<sub>4</sub> MMIP NPs; peroxidase-like catalytic activity; colorimetric chemosensor; norfloxacin detection



**Citation:** Li, M.; Luo, L.; Li, J.; Xiong, Y.; Wang, L.; Liu, X. Colorimetric Chemosensor Based on Fe<sub>3</sub>O<sub>4</sub> Magnetic Molecularly Imprinted Nanoparticles for Highly Selective and Sensitive Detection of Norfloxacin in Milk. *Foods* **2023**, *12*, 285. <https://doi.org/10.3390/foods12020285>

Academic Editor: Thierry Noguere

Received: 1 December 2022

Revised: 3 January 2023

Accepted: 4 January 2023

Published: 7 January 2023



**Copyright:** © 2023 by the authors. Licensee MDPI, Basel, Switzerland. This article is an open access article distributed under the terms and conditions of the Creative Commons Attribution (CC BY) license (<https://creativecommons.org/licenses/by/4.0/>).

## 1. Introduction

Norfloxacin (NOR) was the first discovered fluoroquinolone antibiotic [1] and is widely used in the treatment of human and animal respiratory, digestive, and urinary tract systems [2]. Long-term use of NOR can easily induce bacterial resistance, allergic reactions, or serious harm, such as the “three-cause” effect (carcinogenic, teratogenic, and mutagenic) on the human body. Notably, NOR will increase human resistance to drugs and induce clinical treatment difficulties, which are serious threats to public health. In 2005, the European Union regulated that the maximum residue level of NOR in animal products must not exceed 0.1 ppm [3]. In 2015, the Ministry of Agriculture of the People’s Republic of China issued regulations on the suspension of production, operations, and usage of NOR in animal products in announcement no. 2292 [4]. However, food safety problems caused by the residuals of NOR in animal-derived foods still exist. Therefore, the determination of NOR residue has become an important task in food safety.

The reported detection methods of NOR, such as chromatography [5,6], biosensors [7], and an enzyme-linked immunosorbent assay (ELISA) [8] are usually expensive and time-consuming; moreover, the sample pretreatment is complicated. Furthermore, the practical applications of the biosensor and ELISA methods are severely restricted because the natural enzymes they need are usually too complex to prepare and purify, poor in stability, and expensive. To overcome these shortcomings, researchers have found a series of mimetic enzymes that show similar catalytic activity with natural enzymes [9] and even higher stability than natural enzymes, such as cyclodextrin, crown ethers, and porphyrins. Nevertheless, there are still some problems to be solved, such as the low catalytic efficiency and complex synthesis process.

The new generation of mimetic enzymes (nanozymes) [10–13] can overcome some shortcomings of mimetic enzymes. At present, more nanomaterials with peroxidase-like catalytic activities are used as nanozymes, such as vanadium pentoxide [14], copper oxide [15], manganese dioxide [16], cobalt tetroxide [17,18], cerium oxide [19], and precious metals, such as platinum [20], gold [21], etc. Among them, Fe<sub>3</sub>O<sub>4</sub> magnetic nanoparticles (Fe<sub>3</sub>O<sub>4</sub> NPs) are favored by researchers due to their dual catalytic properties of both peroxidase (POD) and catalase (CAT), as well as good stability and superparamagnetism.

In recent years, the colorimetric method based on Fe<sub>3</sub>O<sub>4</sub> NPs has attracted much attention. For example, the colorimetric method based on Fe<sub>3</sub>O<sub>4</sub> NPs showed high sensitivity and selectivity toward glutathione [22]. The colorimetric method for the detection of *S. typhimurium*, based on Fe<sub>3</sub>O<sub>4</sub> NPs and DNA aptamers, is cost-effective, simple, and able to visibly detect bacteria up to  $7.5 \times 10^5$  CFU/mL [23]. The colorimetric method based on vitamin C (V<sub>C</sub>)-functionalized Fe<sub>3</sub>O<sub>4</sub> NPs (VcFe<sub>3</sub>O<sub>4</sub> NPs) exhibits good sensitivity in detecting H<sub>2</sub>O<sub>2</sub> and glucose as low as 0.29 and 0.288 μmol/L, respectively [24]. However, Fe<sub>3</sub>O<sub>4</sub> NPs are still restricted to specific analytes, require coupled antibodies, or need complex sample pretreatments.

Magnetic molecularly imprinted polymer nanoparticles (MMIP NPs) are developed via MNPs combined with molecularly imprinted polymers (MIPs), which show peroxidase-like catalytic activity, specific adsorption, and magnetic separation ability. MMIP NPs have been successfully applied in the colorimetric sensor. Kong et al. [25] constructed a paper-based colorimetric sensor for the detection of bisphenol A (BPA) based on the peroxidase-like catalytic activity of ZnFe<sub>2</sub>O<sub>4</sub> and cellulose paper wrapped with MIPs. Fan et al. [26] fabricated MIP PtPd nanoflowers with peroxidase-like catalytic activity for selective recognition and detection of H<sub>2</sub>O<sub>2</sub> and glucose. Guo et al. [27] developed a selective analytical method for puerarin by enwrapping a PtCu/PSS-Gr nanocomposite with MIPs and combining it with the high peroxidase-like catalytic activity of PtCu/PSS-Gr. Therefore, MMIP NPs will provide new possibilities in the application of Fe<sub>3</sub>O<sub>4</sub> NPs.

In this work, a new colorimetric chemosensor for NOR detection was constructed based on Fe<sub>3</sub>O<sub>4</sub> MMIP NPs. Fe<sub>3</sub>O<sub>4</sub> MMIP NPs were synthesized based on Fe<sub>3</sub>O<sub>4</sub> NPs as magnetic carriers by surface imprinting technology, and their peroxidase-like catalytic activities were examined. The experimental conditions of detecting NOR were optimized. The detection performance of the colorimetric chemosensor was explored. Moreover, the applicability of the colorimetric chemosensor was demonstrated by detecting NOR in milk and compared with the ELISA method. The contrasted colorimetric chemosensor method proved to be simple, fast, low-cost, and efficient for NOR detection in foods.

## 2. Materials and Methods

### 2.1. Reagents and Instruments

Norfloxacin (NOR), ciprofloxacin (CIP), enrofloxacin (ENR), and danofloxacin (DAN) were purchased from Shanghai Yuanye Bio-Chem Technology Co., Ltd. (Shanghai, China) and the purity was >98%. Tetramethyl ammonium hydroxide (TMAOH) and (3-Aminopropyl) triethoxysilane (APTES) were purchased from Shanghai Aladdin Bio-Chem Technology Co., Ltd. (Shanghai, China). Dopamine (DA), tetracycline hydrochloride (TC), and sulfadiazine (SD) were purchased from Shanghai Aladdin Bio-Chem Technology Co., Ltd. (Shanghai, China), and the purity was >98%. TMB, OPD, and ABTS were purchased from Shanghai Macklin Bio-Chem Co., Ltd. (Shanghai, China) and the purity was >99%. A NOR ELISA Kit (RN 45S) was purchased from Shenzhen Rongjin Technology Co., Ltd. All chemicals and solvents were of a commercially available analytical reagent grade; double distilled water was used throughout this work.

The milk samples were natural pure milk purchased from Inner Mongolia Mengniu Dairy (Group) Limited by Share, Ltd., natural pure milk purchased from Inner Mongolia Yili Industrial Group Limited by Share, Ltd., and deluxe milk purchased from Inner Mongolia Mengniu Dairy (Group) Limited by Share, Ltd.

The absorbance spectrum was obtained by a multi-mode microplate spectrophotometer (Multiskan GO 1510, Thermo Fisher Scientific, Waltham, MA, USA).

### 2.2. Synthesis of Fe<sub>3</sub>O<sub>4</sub> MMIP NPs

Fe<sub>3</sub>O<sub>4</sub> MMIP NPs were prepared according to the procedure that our group previously established [28]. Briefly, FeCl<sub>3</sub>·6H<sub>2</sub>O and FeCl<sub>2</sub>·4H<sub>2</sub>O were mixed and heated under nitrogen gas protection. Then, 40 mL of NaOH (2 mol/L) was added, and this mixture was stirred (550 rpm, 1 h, 80 °C). Fe<sub>3</sub>O<sub>4</sub> NPs were dissolved in TMAOH solution (7%), followed by 2 h of incubation; they were then dissolved in a 120 mL solution of ethanol–water (1:1, *v/v*) (containing 100 mM Tris-HCl, pH = 8.5). Subsequently, 3 mL of APTES was added and this mixture was stirred (40 °C, 350 rpm, 10 h). A total of 500 mg of APTES-modified Fe<sub>3</sub>O<sub>4</sub> NP was dissolved in 100 mL of ethanol–water (1:1, pH = 8.5). After ultrasonic treatment (25 °C, 10 min), 15 mg of NOR and 135 mg of DA were added to the flask. The mixture was stirred (350 rpm, 3 h, 25 °C). Then, the Fe<sub>3</sub>O<sub>4</sub> MMIP NPs were separated, dried in a vacuum (60 °C, 24 h), and stored at 4 °C. Meanwhile, the Fe<sub>3</sub>O<sub>4</sub> magnetic non-imprinting polymer nanoparticles (Fe<sub>3</sub>O<sub>4</sub> MMIP NPs) were prepared without the template molecule as a control.

### 2.3. Peroxidase-Like Catalytic Activity of Fe<sub>3</sub>O<sub>4</sub> MMIP NPs

Chromogenic agents were examined through the Fe<sub>3</sub>O<sub>4</sub> MMIP NP catalytic oxidation experiment: 200 µL of Fe<sub>3</sub>O<sub>4</sub> MMIP NPs (4 mg/mL), 100 µL of ultrapure water, 400 µL of HAc-NaAc (0.2 M), 250 µL of H<sub>2</sub>O<sub>2</sub> (0.06 M), and 50 µL of a substrate (0.008 M TMB, OPD or ABTS) was mixed and incubated for 4 min at 25 °C. The supernatant was separated, then its absorbance spectrum was measured by a multi-mode microplate spectrophotometer.

The feasibility of the Fe<sub>3</sub>O<sub>4</sub> MMIP NPs for NOR detection was verified by investigating the absorbance difference ( $\Delta A$ ) of the Fe<sub>3</sub>O<sub>4</sub> MMIP NP-H<sub>2</sub>O<sub>2</sub>-TMB reaction system before and after the addition of NOR. A total of 100 µL of NOR (0.01 mg/mL) or ultrapure water was added to 200 µL of Fe<sub>3</sub>O<sub>4</sub> MMIP NPs/Fe<sub>3</sub>O<sub>4</sub> MMIP NPs (4 mg/mL) and stirred for 15 min in a constant temperature incubator. The supernatant was separated, then its absorbance spectrum was measured via a multi-mode microplate spectrophotometer.

### 2.4. In Situ Colorimetric Measurement

The effects of the buffer type (NaAc, HAc-NaAc, Na<sub>2</sub>HPO<sub>4</sub>-CA, or Na<sub>2</sub>HPO<sub>4</sub>-NaH<sub>2</sub>PO<sub>4</sub>), pH (2–6), H<sub>2</sub>O<sub>2</sub> concentration (0.004–2 M), the volume ratio of TMB (0.008 M) to H<sub>2</sub>O<sub>2</sub> (0.1 M) (1:1, 1:2, 1:3, 1:4, 4:1, 3:1, and 2:1), and reaction time (1, 2, 3, 4, 6, 8, 10, 12, and 14 min) on the catalytic activity of Fe<sub>3</sub>O<sub>4</sub> MMIP NPs were investigated. Under the optimal catalytic activity conditions, the colorimetric detection of NOR based on the Fe<sub>3</sub>O<sub>4</sub> MMIP NPs was achieved. Moreover, 10 µL of a standard solution containing different concentrations of NOR was separately incubated with 200 µL of Fe<sub>3</sub>O<sub>4</sub> MMIP NPs. Then, 200 µL of HAc-NaAc, 400 µL of H<sub>2</sub>O<sub>2</sub>, and 100 µL of TMB were added. The mixture was incubated for 4 min at 25 °C. The supernatant was then separated and the absorbance intensity at 652 nm was measured by a multi-mode microplate spectrophotometer. The selectivity experiments were carried out using 100 µL of a standard solution of NOR, CIP, ENR, DAN, SD, and TC, with an initial concentration of 200 ng/mL. Reproducibility experiments were also carried out in the same procedure. In the reproducibility experiments, the Fe<sub>3</sub>O<sub>4</sub> MMIP NPs were separated by a magnet and washed twice with 1 mL of ultrapure water.

### 2.5. Preparation of Milk Samples

The milk samples were purchased from a local supermarket. A total of 1 mL of milk was vortically mixed with 8 mL of an EDTA-McIlvaine buffer solution (1000 r/min, 1 min), followed by an ultrasonic for 10 min (25 °C, 60 Hz), and centrifugated for 10 min (10,000 r/min, 4 °C). Then the supernatant with different concentrations of NOR (10, 50, and 100 ng/mL) was prepared for the recovery experiments. The absence of NOR in the

milk sample was confirmed by high-performance liquid chromatography-tandem mass spectrometry (GB/T21312-2007, China).

### 2.6. Calculation of LOD

According to the rules of the International Union of Pure and Applied Chemistry (IUPAC):  $C_L = k \times S_b/m$  ( $C_L$  means the detection limit;  $k$  means the confidence factor;  $m$  means the slope of the standard curve in the low concentration range;  $S_b$  means the standard deviation of a blank).

## 3. Results and Discussion

### 3.1. The Kinetic Parameters of TMB Oxidation Catalyzed by $Fe_3O_4$ MMIP NPs

In order to explain the peroxidase-like catalytic activity of  $Fe_3O_4$  MMIP NPs and construct a colorimetric chemosensor, the kinetic parameters of TMB oxidation catalyzed by  $Fe_3O_4$  MMIP NPs were determined. The initial reaction velocity was calculated according to the Michaelis–Menten equation:  $v = V_{max} [S]/(K_m + [S])$  ( $v$  is the initial reaction velocity,  $V_{max}$  is the maximum reaction rate,  $[S]$  is the substrate concentration,  $K_m$  is the Michaelis constant.) The relationship between the  $H_2O_2$  concentration (or the TMB concentration) and the reaction rate was obtained using the double-reciprocal mapping method.

Michaelis–Menten curves were obtained (Figure S2, Supporting Information).  $K_m$  and  $V_{max}$  were obtained by the Lineweaver–Burk plot (Table 1). The  $K_m$  of  $Fe_3O_4$  MMIP NPs to TMB and  $H_2O_2$  (0.088 mM and 0.16 mM, respectively) was smaller than that of HRP [28], indicating that the affinity of  $Fe_3O_4$  MMIP NPs for TMB and  $H_2O_2$  was higher than that of HRP, and  $Fe_3O_4$  MMIP NPs could catalyze the oxidation of TMB faster than HRP. Compared with other Fe-based nanomaterials [24,29–32], the  $Fe_3O_4$  MMIP NPs in this work also showed relatively high affinity and a maximum reaction rate to TMB and  $H_2O_2$ . The reason may be that small particle sizes, large selective surface areas, and rich surface charges were easily able to adsorb positively charged TMB and had a high affinity for TMB [33].

**Table 1.**  $K_m$  and  $V_{max}$  of HRP and nanomaterials.

Catalyst	$K_m/mM$		$V_{max}/10^{-8} M s^{-1}$		References
	TMB	$H_2O_2$	TMB	$H_2O_2$	
HRP	0.434	3.7	10	8.7	[28]
$Fe_3O_4$	0.098	154	3.44	9.78	[29]
$Fe_3O_4$ NPs	0.313	0.013	13.35	2.95	[30]
Fe-COF	0.02	0.143	3.83	4.74	[31]
Vc $Fe_3O_4$ NPs	0.067	2.96	1.93	2.05	[24]
$Fe_3O_4$ - $MnO_2$	0.101	0.041	0.57	2.94	[32]
$Fe_3O_4@C$	0.27	0.035	12	3.34	[28]
MMIP NPs	0.088	0.16	3.44	6.25	This work

### 3.2. Detection Feasibility

TMB, o-phenylenediamine (OPD), and 2,2'-diazobis(3-ethylbenzothiazoline-6-sulfonic acid) (ABTS) were used to verify the peroxidase-like catalytic activity of  $Fe_3O_4$  MMIP NPs (Figure 1A). In the participation of  $H_2O_2$ ,  $Fe_3O_4$  MMIP NPs could catalyze the oxidation of TMB, OPD, and ABTS, which made the solution appear blue, yellow, and green, respectively. The above results indicate that  $Fe_3O_4$  MMIP NPs has peroxidase-like catalytic activity. The absorbance of the  $Fe_3O_4$  MMIP NPs- $H_2O_2$ -TMB reaction system at the optimal absorption wavelength (652 nm) is much more obvious than that of the  $Fe_3O_4$  MMIP NPs- $H_2O_2$ -OPD reaction system (450 nm) and  $Fe_3O_4$  MMIP NPs- $H_2O_2$ -ABTS reaction system (415 nm or 734 nm). Therefore, TMB was selected as the chromogenic agent for  $Fe_3O_4$  MMIP NPs.

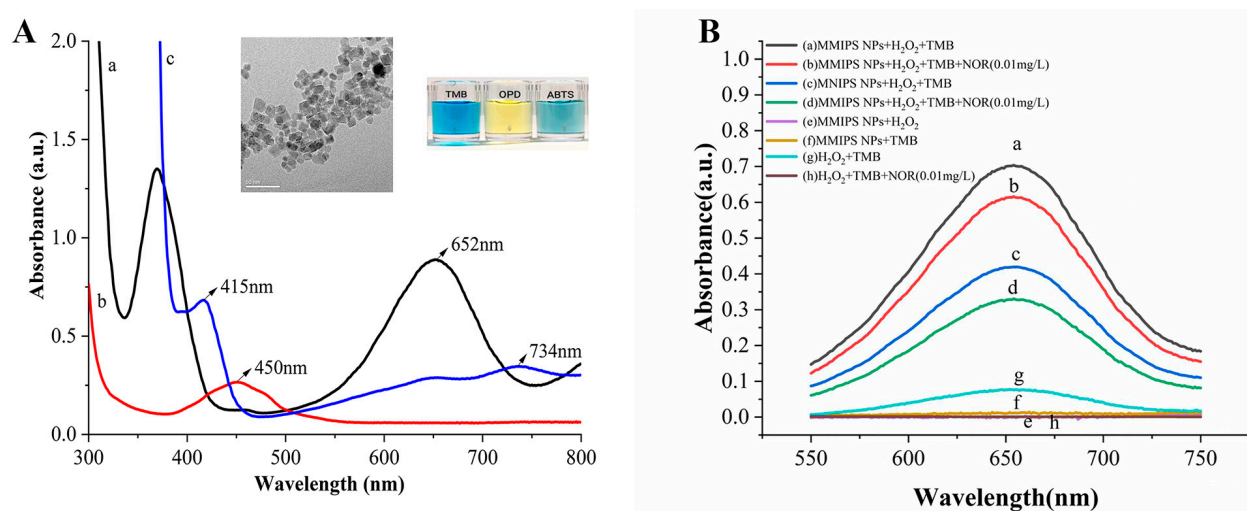


**Figure 1.** Detection feasibility of Fe<sub>3</sub>O<sub>4</sub> MMIP NPs for NOR. (A) Absorption spectra of the reactions of different chromogenic substrates, a: TMB, b: OPD, and c: ABTS. (B) Absorption spectra of different reaction systems a: Fe<sub>3</sub>O<sub>4</sub> MMIP NPs + H<sub>2</sub>O<sub>2</sub> + TMB, b: Fe<sub>3</sub>O<sub>4</sub> MMIP NPs + H<sub>2</sub>O<sub>2</sub> + TMB + 0.01 mg/mL NOR, c: Fe<sub>3</sub>O<sub>4</sub> MMIP NPs + H<sub>2</sub>O<sub>2</sub> + TMB, d: Fe<sub>3</sub>O<sub>4</sub> MMIP NPs + H<sub>2</sub>O<sub>2</sub> + TMB + 0.01 mg/mL NOR, e: Fe<sub>3</sub>O<sub>4</sub> MMIP NPs + H<sub>2</sub>O<sub>2</sub>, f: Fe<sub>3</sub>O<sub>4</sub> MMIP NPs + TMB, g: H<sub>2</sub>O<sub>2</sub> + TMB, h: H<sub>2</sub>O<sub>2</sub> + TMB + 0.01 mg/mL NOR. All trials were repeated 3 times.

Then, the feasibility of the NOR detection of the constructed colorimetric chemosensor was verified by catalyzing the oxidation of colorless TMB into a blue product (oxTMB). As shown in Figure 1B, when there were only Fe<sub>3</sub>O<sub>4</sub> MMIP NPs or H<sub>2</sub>O<sub>2</sub> in the reaction system, no absorbance at 652 nm could be observed and the solution was colorless, which indicated that TMB can only be oxidized when Fe<sub>3</sub>O<sub>4</sub> MMIP NPs and H<sub>2</sub>O<sub>2</sub> exist simultaneously (curve e, curve f, and curve g). Compared with curve g, curve h showed no absorbance at 652 nm; this might be caused by the direct inhibiting effect of NOR on the TMB-H<sub>2</sub>O<sub>2</sub> reaction. On the contrary, when Fe<sub>3</sub>O<sub>4</sub> MMIP NPs, TMB, and H<sub>2</sub>O<sub>2</sub> existed, the absorbance of the reaction system at 652 nm was greatly enhanced (curve a), which indicated that Fe<sub>3</sub>O<sub>4</sub> MMIP NPs had high peroxidase-like catalytic activity to catalyze the oxidation of TMB in the participation of H<sub>2</sub>O<sub>2</sub>. When NOR was added to the reaction system, the absorbance at 652 nm was reduced (curve b) and the solution color became lighter, indicating that the presence of NOR inhibited the peroxidase-like catalytic activity of Fe<sub>3</sub>O<sub>4</sub> MMIP NPs. The reason was that NOR could selectively bind to the cavity in the surface of Fe<sub>3</sub>O<sub>4</sub> MMIP NPs, which reduced the contact area of the H<sub>2</sub>O<sub>2</sub> and Fe<sub>3</sub>O<sub>4</sub> MMIP NPs. As a comparison, the peroxidase-like catalytic activity of Fe<sub>3</sub>O<sub>4</sub> MMIP NPs was also tested. Compared with curve c, the absorbance peak intensity of curve d was lower. This may have been caused by unselective binding between NOR and Fe<sub>3</sub>O<sub>4</sub> MMIP NPs. It is worth noting that the absorption peak intensities of curve c and curve d were lower than those of curve a and curve b, indicating that the peroxidase-like catalytic activities of Fe<sub>3</sub>O<sub>4</sub> MMIP NPs were lower than those of Fe<sub>3</sub>O<sub>4</sub> MMIP NPs. Due to the lack of selective cavities on the surfaces of Fe<sub>3</sub>O<sub>4</sub> MMIP NPs, a barrier was formed between H<sub>2</sub>O<sub>2</sub> and Fe<sub>3</sub>O<sub>4</sub> MMIP NPs, which hindered the catalysis of Fe<sub>3</sub>O<sub>4</sub> MMIP NPs to the substrate. All of the above results indicate that the Fe<sub>3</sub>O<sub>4</sub> MMIP NPs-H<sub>2</sub>O<sub>2</sub>-TMB reaction system has feasibility for the colorimetric detection of NOR.

### 3.3. Optimization of the Experimental Conditions

Buffer types affected the peroxidase-like catalytic activities of Fe<sub>3</sub>O<sub>4</sub> MMIP NPs greatly (Figure 2A). The highest absorbance was observed in HAc-NaAc (0.2 M). We speculated that the concentration change of H<sup>+</sup> promoted the dissociation of H<sub>2</sub>O<sub>2</sub>, which accelerated

the oxidation rate of TMB. Therefore, HAc-NaAc (0.2 M) was selected as the buffer for the reaction system.

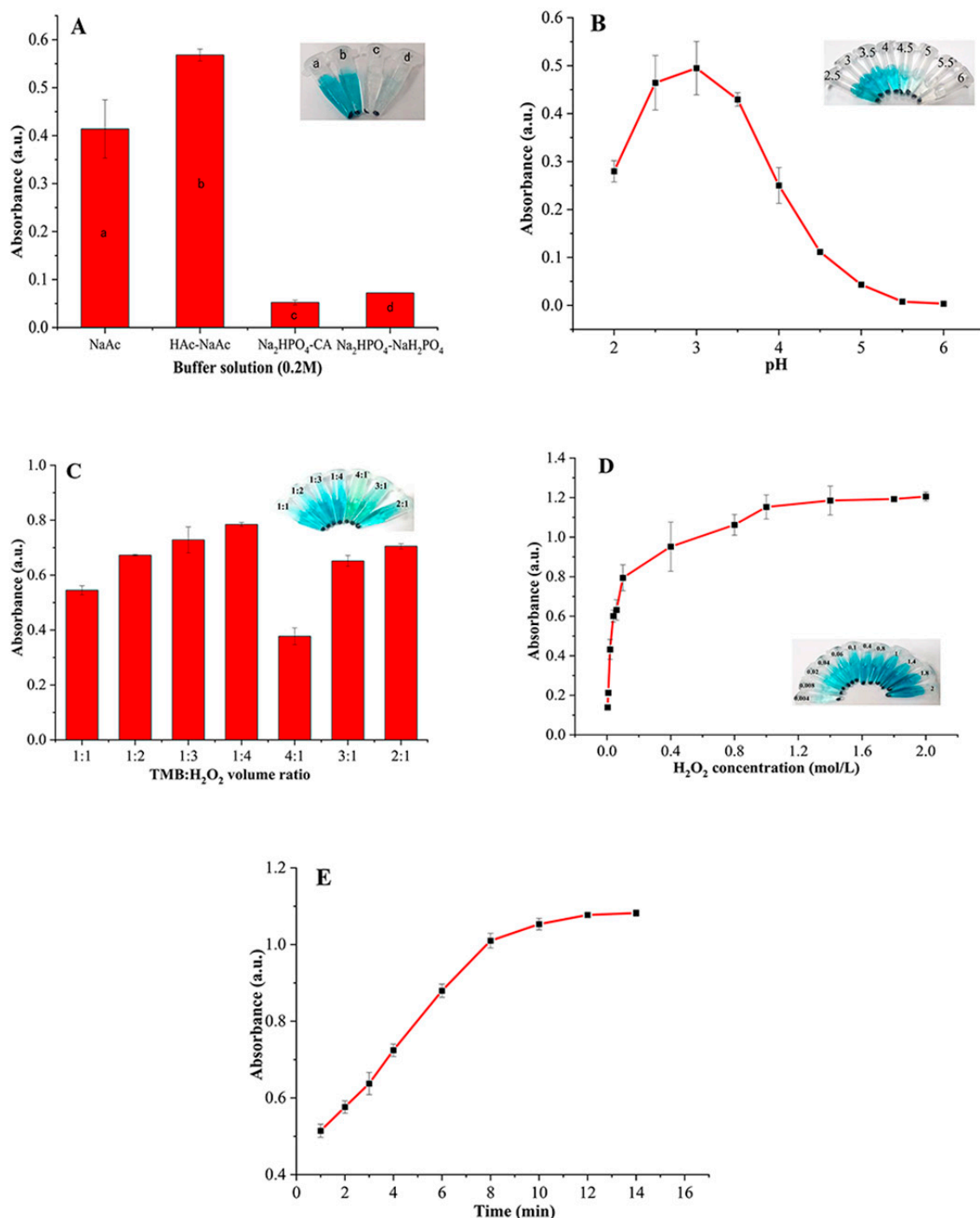


**Figure 2.** The influences of different factors on the performances of Fe<sub>3</sub>O<sub>4</sub> MMIP NPs. (A) Buffer type, 0.2 M buffer pH = 3.5, 250  $\mu$ L 0.06 M H<sub>2</sub>O<sub>2</sub>, 50  $\mu$ L 0.008 M TMB, reaction time 4 min; (B) pH, 0.2 M HAc-NaAc, 250  $\mu$ L 0.06 M H<sub>2</sub>O<sub>2</sub>, 50  $\mu$ L 0.008 M TMB, reaction time 4 min; (C) TMB/H<sub>2</sub>O<sub>2</sub> volume ratio, 0.2 M HAc-NaAc pH = 3.5, 0.06 M H<sub>2</sub>O<sub>2</sub>, 0.008 M TMB, reaction time 4 min; (D) H<sub>2</sub>O<sub>2</sub> concentration, 0.2 M HAc-NaAc pH = 3.5, 250  $\mu$ L H<sub>2</sub>O<sub>2</sub>, 50  $\mu$ L 0.008 M TMB, reaction time 4 min; (E) Reaction time, 0.2 M HAc-NaAc pH = 3.5, 250  $\mu$ L 0.06 M H<sub>2</sub>O<sub>2</sub>, 50  $\mu$ L 0.008 M TMB. All trials were repeated 3 times.

The effect of pH on the peroxidase-like catalytic activity of Fe<sub>3</sub>O<sub>4</sub> MMIP NPs was examined by the buffer within the pH range of 2–6. Figure 2B shows the pH-dependent response curve. When pH < 3, the absorbance of the reaction system increased, accompanied by the increase of the pH, while the further increasing pH resulted in a decrease of the absorbance intensity. Therefore, pH = 3 was selected as the condition for the reaction system.

The TMB/H<sub>2</sub>O<sub>2</sub> volume ratio also had a great effect on the peroxidase-like catalytic activity of Fe<sub>3</sub>O<sub>4</sub> MMIP NPs (Figure 2C). The absorbance of the reaction system increased with the increase of the H<sub>2</sub>O<sub>2</sub> volume, and the absorbance reached the maximum when the volume ratio of TMB/H<sub>2</sub>O<sub>2</sub> was 1:4. When the volume of H<sub>2</sub>O<sub>2</sub> was fixed, the volume of TMB increased, and the absorbance value showed a decreasing trend. Therefore, the volume ratio of TMB to H<sub>2</sub>O<sub>2</sub> was chosen as 1:4 for the reaction system.

The influence of the H<sub>2</sub>O<sub>2</sub> concentration on the peroxidase-like catalytic activity of Fe<sub>3</sub>O<sub>4</sub> MMIP NPs was studied and the results are shown in Figure 2D. With the increase of the H<sub>2</sub>O<sub>2</sub> concentration (<0.1 M), the absorbance increased rapidly. When the concentration of H<sub>2</sub>O<sub>2</sub> was 0.1 M, the absorbance value was 0.7943 and the solution color changed significantly in a short time, which was easy to be recognized by the naked eye. When the concentration was more than 0.1 M, the increase rate decreased and gradually leveled off, and the color change with the concentration of H<sub>2</sub>O<sub>2</sub> was not obvious. Moreover, 0.1 M H<sub>2</sub>O<sub>2</sub> was chosen for the reaction system.

The reaction time of the Fe<sub>3</sub>O<sub>4</sub> MMIP NPs-H<sub>2</sub>O<sub>2</sub>-TMB system was examined from 1 to 14 min. The absorbance increased gradually when the reaction time was prolonged (Figure 2E). When the reaction time was 4 min, the solution color changed sufficiently (it could be recognized by the naked eye). Considering the purpose of rapid detection, 4 min was chosen as the reaction time for the reaction system.

### 3.4. In Situ Colorimetric Measurements

Under the optimized experimental conditions, different concentrations of NOR were detected by the constructed colorimetric chemosensor based on Fe<sub>3</sub>O<sub>4</sub> MMIP NPs. As can be seen in Figure 3A, with the increase in the NOR concentration, the absorbance of the reaction system at 652 nm gradually decreased. This indicated that NOR inhibited the production of oxTMB. There are two main reasons. First, NOR occupied the cavities on the surface of Fe<sub>3</sub>O<sub>4</sub> MMIP NPs and prevented the contact between H<sub>2</sub>O<sub>2</sub> and Fe<sub>3</sub>O<sub>4</sub> MMIP NPs, which partially decreased the peroxidase-like catalytic activity of Fe<sub>3</sub>O<sub>4</sub> MMIP NPs. Second, there was a direct inhibiting effect of NOR on the TMB-H<sub>2</sub>O<sub>2</sub> reaction. Figure 3B shows a good linear relationship between the  $\Delta A$  (652 nm) and NOR concentration in the range of 10–300 ng/mL. The linear regression equation was  $Y = 0.000947x + 0.03176$  ( $R^2 = 0.9878$ ), and the detection limit was 9 ng/mL.

To evaluate the selectivity of the colorimetric chemosensor, the structural analogs (CIP, ENR, and DAN) and nonstructural analogs (SD and TC) were selected as interfering antibiotics. Figure 3C shows the  $\Delta A$  of the Fe<sub>3</sub>O<sub>4</sub> MMIP NPs-H<sub>2</sub>O<sub>2</sub>-TMB reaction system with and without NOR, CIP, ENR, DAN, SD, and TC (the final concentration of each component was 200 ng/mL). The  $\Delta A$  of the colorimetric chemosensor for NOR detection was the largest (1.77 times, 2.27 times, 2.67 times, 6.41 times, and 11.42 times for CIP, ENR, DAN, SD, and TC, respectively). This is because Fe<sub>3</sub>O<sub>4</sub> MMIP NPs could selectively adsorb NOR. The results clearly demonstrate the selectivity of the Fe<sub>3</sub>O<sub>4</sub> MMIP NP-based colorimetric chemosensor. In addition, the  $\Delta A$  of the Fe<sub>3</sub>O<sub>4</sub> MMIP NPs-H<sub>2</sub>O<sub>2</sub>-TMB reaction system was less than that of the Fe<sub>3</sub>O<sub>4</sub> MMIP NPs-H<sub>2</sub>O<sub>2</sub>-TMB system under the same conditions. This was mainly because the Fe<sub>3</sub>O<sub>4</sub> MMIP NPs failed to form molecular imprint cavities, and there was only a small amount of non-selective adsorption.

The reusability assay (Figure 3D) showed that the catalytic activities of Fe<sub>3</sub>O<sub>4</sub> MMIP NPs remained above 86% after 6 cycles of colorimetric detection, indicating that the Fe<sub>3</sub>O<sub>4</sub> MMIP NP-based colorimetric chemosensor had good stability. Xiong et al. [34] revealed that no loss of activity was observed after 10 cycles of the magnetic core-shell nanoflower Fe<sub>3</sub>O<sub>4</sub>@MnO<sub>2</sub>. The difference might have been induced by the synthesis method. However,

Lian et al. [35] reported that when the relative activity was more than 80%, the suitable stability was good.

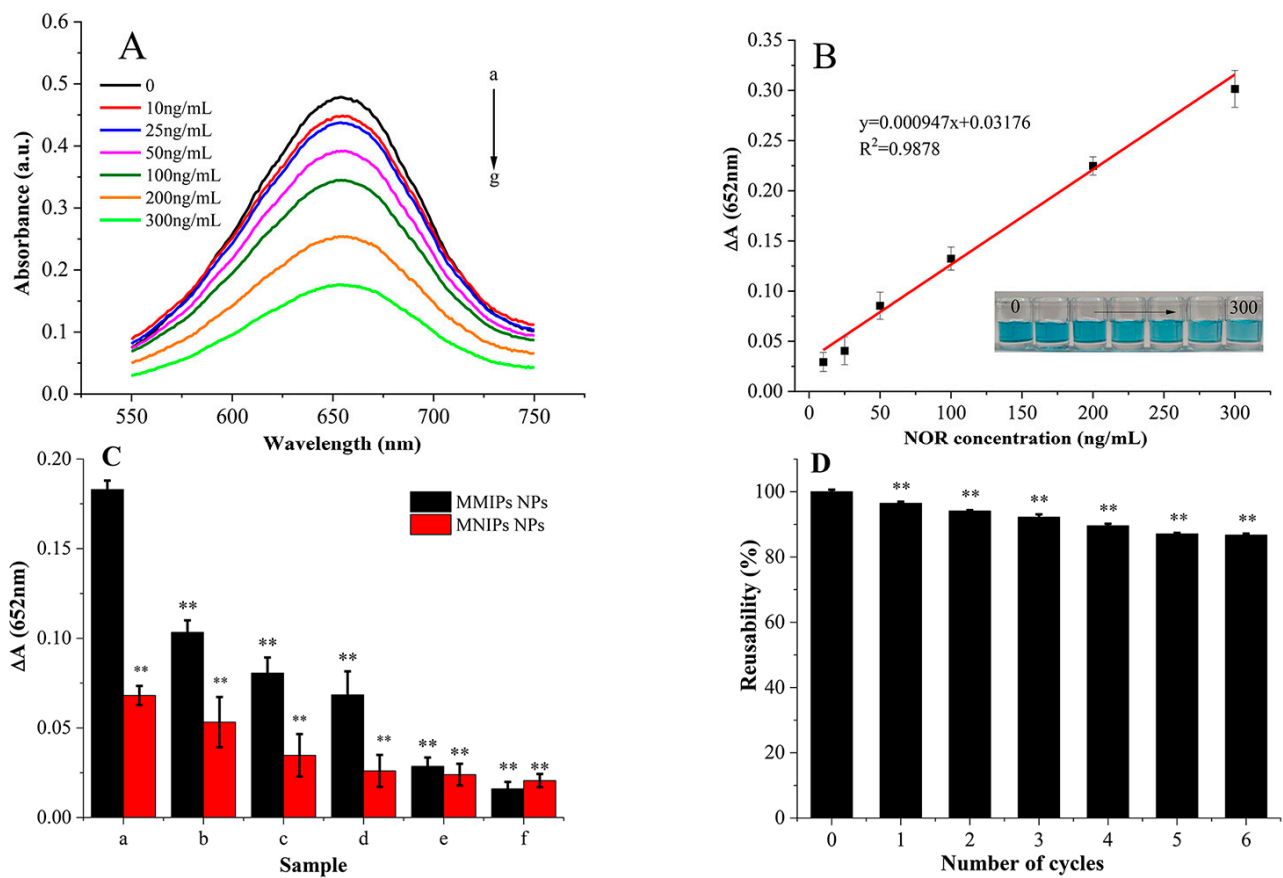


**Figure 3.** In situ colorimetric measurements. (A) Absorption spectra of oxTMB at different NOR concentrations (a–g: 0, 10, 25, 50, 100, 200, and 300 ng/mL). (B) Linear relationship between the  $\Delta A$  (652 nm) and NOR concentrations. (C) The selectivity of the colorimetric chemosensor at 25 °C (a: NOR, b: CIP, c: ENR, d: DAN, e: SD, f: TC, with the initial concentration of 0.02 mg/mL), \*\* significantly different compared with MMIP NPs to NOR,  $p < 0.01$ . (D) The reusability of the  $\text{Fe}_3\text{O}_4$  MMIP NPs for NOR, \*\* significantly different compared to the first time used,  $p < 0.01$ . All trials were repeated 3 times.

### 3.5. Detection of NOR in Milk

After the pretreatment of three different milk samples, the constructed colorimetric chemosensor was applied to detect the NOR residuals in the samples. The results (shown in Figure S1 (Supporting Information)) show that no response signal ( $\Delta A$ ) was obtained, indicating that there were no NOR residues in the samples, which was consistent with the results of the ELISA kit (the detected NOR concentrations in three milk samples were  $-0.0906$  ng/mL,  $-0.1660$  ng/mL, and  $-0.1376$  ng/mL, respectively).

The recovery experiments showed that the recovery range of the established colorimetric method was 78.29% to 95.81%, and the relative standard deviation (RSD) ranged from 3.47% to 9.88% (Table 2). The constructed colorimetric chemosensor had good reliability and the detection time was short (only 30 min). The results above prove that this colorimetric chemosensor can be used for the rapid determination of NOR residue in milk.



**Table 2.** Recovery rate experiment results for milk spiked with NOR ( $n = 3$ ).

Milk Sample	Spiked (ng/mL)	Detected (ng/mL)	Recovery (%)	RSD (%)
1	10.00	8.98	89.83	4.32
	50.00	42.74	85.48	3.47
	100.00	78.29	78.29	9.35
2	10.00	9.09	90.88	9.46
	50.00	44.53	89.07	6.36
	100.00	82.83	82.83	3.89
3	10.00	9.58	95.81	9.88
	50.00	41.15	82.31	6.64
	100.00	83.71	83.71	4.22

### 3.6. Comparison of Detection Methods for NOR

The colorimetric chemosensor was compared with other methods for NOR detection in animal-derived foods (Table 3). While HPLC analysis [36], HPLC with fluorescence [37], ELISA method [38], the fluorescence analysis [8,39,40], and Raman spectroscopy [41] improved the sensitivity and accuracy for NOR detection, they increased the testing costs as well as the requirements for operators. Moreover, the antibodies used in the ELISA method increased the testing costs, and the probe based on quantum dots used in the fluorescence analysis made the procedure much more complex. Xie et al. [42] proposed a rapid method for the preparation of novel MIPs with covalent organic frameworks as support for the selective recognition of NOR. However, the synthesis of MIPs with covalent organic frameworks is complex, the separation of MIPs from the samples needs centrifugation, and the quantitative analysis needs an HPLC analysis.

**Table 3.** Comparison of detection methods for NOR.

Method	Sample	Linear Ranges (ng/mL)	LOD (ng/mL)	Recovery (%)	Reference
HPLC analysis	Milk	$1 \times 10^3$ – $30 \times 10^3$	260.0	99.50–101.20	[36]
HPLC with fluorescence	chicken tissues	$10$ – $1 \times 10^3$	2.5	79.20–93.40	[37]
ELISA method	water	0.1–10	0.016	74–105	[38]
Fluorescence analysis	Fish, milk	1–90	0.80	90.92–111.53	[39]
Fluorescence analysis based on immunoassay	Milk	13–3986	0.0034	86.44–101.30	[8]
Fluorescence analysis based on time-resolved methodology	Milk	0.5–1000	0.14	91.90–110.50	[40]
Raman spectroscopy	Milk	7.98–159.67	1.701	101.29–104.00	[41]
Colorimetric chemosensor based on Fe <sub>3</sub> O <sub>4</sub> MMIP NPs	Milk	10–300	8.90	75.97–95.81	This work

Compared with the studies above, the colorimetric chemosensor in this work showed several obvious advantages. First, the separation of Fe<sub>3</sub>O<sub>4</sub> MMIP NPs from samples by magnets was quick. Second, the Fe<sub>3</sub>O<sub>4</sub> MMIP NPs could selectively absorb NOR from samples and had good stability. Third, the sample pretreatment was perfectly combined with colorimetric detection making the whole procedure simple. Finally, the visual qualitative analysis could be achieved by the color change while quantitative analysis could be realized via simple instruments. Therefore, the colorimetric chemosensor could offer a better way for NOR detection in food.

#### 4. Conclusions

In summary, a new colorimetric chemosensor for in situ detection of NOR based on the peroxidase-like catalytic activities of Fe<sub>3</sub>O<sub>4</sub> MMIP NPs was constructed. Fe<sub>3</sub>O<sub>4</sub> MMIP NPs have highly selective absorption abilities, excellent catalytic performances, and good stability for NOR detection. The detection procedure and the sample pretreatment are simple. This method has been successfully applied for the selective recognition and determination of NOR residue in milk and the result is consistent with the ELISA kit. The established method can provide a reliable strategy for the simple, fast, and precise detection of NOR residue in milk.

**Supplementary Materials:** The following supporting information can be downloaded at <https://www.mdpi.com/article/10.3390/foods12020285/s1>, Figure S1: Fe<sub>3</sub>O<sub>4</sub> MMIP NP colorimetric method for the detection of actual samples; Figure S2: Kinetic analysis of Fe<sub>3</sub>O<sub>4</sub> MMIP NP peroxidase-like catalytic activity.

**Author Contributions:** L.L. and X.L. designed and conceived the study. L.L., J.L., Y.X. and L.W. carried out the experiment. L.L. and J.L. analyzed the data. M.L., L.L. and J.L. prepared the figures. M.L. and X.L. wrote the manuscript. All authors have read and agreed to the published version of the manuscript.

**Funding:** This work was supported by the Natural Science Foundation of Hunan Province (no. 2020JJ4354).

**Data Availability Statement:** All related data and methods are presented in this paper and the Supplementary Materials.

**Conflicts of Interest:** The authors declare no competing financial interests.

#### References

1. Gadebusch, H.H.; Shungu, D.L. Norfloxacin, the First of a New Class of Fluoroquinolone Antimicrobials, Revisited. *Int. J. Antimicrob. Agents* **1991**, *1*, 3–28. [[CrossRef](#)]
2. Wang, Z.; Song, B.; Li, J.; Teng, X. Degradation of Norfloxacin Wastewater Using Kaolin/Steel Slag Particle Electrodes: Performance, Mechanism and Pathway. *Chemosphere* **2021**, *270*, 128652. [[CrossRef](#)]
3. Li, Y.F.; Sheng, Y.J.; Tsao, H.K. Evaporation stains: Suppressing the coffee-ring effect by contact angle hysteresis. *Langmuir* **2013**, *25*, 7802–7811. [[CrossRef](#)]
4. Announcement No. 2292/2015 of the Ministry of Agriculture of the People's Republic of China. *Gazette of the Ministry of Agriculture of the People's Republic of China*. Available online: [http://www.moa.gov.cn/govpublic/SYJ/201509/t20150907\\_4819267.htm](http://www.moa.gov.cn/govpublic/SYJ/201509/t20150907_4819267.htm) (accessed on 1 September 2015).
5. Annunziata, L.; Visciano, P.; Stramenga, A.; Colagrande, M.N.; Campana, G.; Scortichini, G.; Migliorati, G.; Compagnone, D. Development and Validation of a Method for the Determination of Quinolones in Muscle and Eggs by Liquid Chromatography-Tandem Mass Spectrometry. *Food Anal. Methods* **2016**, *9*, 2308–2320. [[CrossRef](#)]
6. Samanidou, V.F.; Demetriou, C.E.; Papadoyannis, I.N. Direct Determination of Four Fluoroquinolones, Enoxacin, Norfloxacin, Ofloxacin, and Ciprofloxacin, in Pharmaceuticals and Blood Serum by HPLC. *Anal. Bioanal. Chem.* **2003**, *375*, 623–629. [[CrossRef](#)]
7. Wang, Z.; Li, J.; Liu, X.; Yang, J.; Lu, X. Preparation of an Amperometric Sensor for Norfloxacin Based on Molecularly Imprinted Grafting Photopolymerization. *Anal. Bioanal. Chem.* **2013**, *405*, 2525–2533. [[CrossRef](#)] [[PubMed](#)]
8. Liu, X.; Xu, Z.; Han, Z.; Fan, L.; Liu, S.; Yang, H.; Chen, Z.; Sun, T.; Ning, B. A Highly Sensitive and Dual-Readout Immunoassay for Norfloxacin in Milk Based on QDs-FM@ALP-SA and Click Chemistry. *Talanta* **2021**, *234*, 122703. [[CrossRef](#)] [[PubMed](#)]
9. Yang, B.; Li, J.; Deng, H.; Zhang, L. Progress of Mimetic Enzymes and Their Applications in Chemical Sensors. *Crit. Rev. Anal. Chem.* **2016**, *46*, 469–481. [[CrossRef](#)] [[PubMed](#)]
10. Manea, F.; Houillon, F.B.; Pasquato, L.; Scrimin, P. Nanozymes: Gold-nanoparticle-based Transphosphorylation Catalysts. *Angew. Chem.* **2004**, *116*, 6291–6295. [[CrossRef](#)]
11. Zhang, X.; Li, G.; Wu, D.; Liu, J.; Wu, Y. Recent Advances on Emerging Nanomaterials for Controlling the Mycotoxin Contamination: From Detection to Elimination. *Food Front.* **2020**, *1*, 360–381. [[CrossRef](#)]
12. Jagtiani, E. Advancements in Nanotechnology for Food Science and Industry. *Food Front.* **2022**, *3*, 56–82. [[CrossRef](#)]
13. Gu, Y.; Li, Y.; Ren, D.; Sun, L.; Zhuang, Y.; Yi, L.; Wang, S. Recent Advances in Nanomaterial-assisted Electrochemical Sensors for Food Safety Analysis. *Food Front.* **2022**, *153*, 112046. [[CrossRef](#)]
14. André, R.; Natálio, F.; Humanes, M.; Leppin, J.; Heinze, K.; Wever, R.; Schröder, H.; Müller, W.E.G.; Tremel, W. V<sub>2</sub>O<sub>5</sub> Nanowires with an Intrinsic Peroxidase-like Activity. *Adv. Funct. Mater.* **2011**, *21*, 501–509. [[CrossRef](#)]

15. Chen, W.; Chen, J.; Liu, A.; Wang, L.; Li, G.; Lin, X. Peroxidase-like Activity of Cupric Oxide Nanoparticle. *ChemCatChem* **2011**, *3*, 1151–1154. [[CrossRef](#)]
16. Liu, X.; Wang, Q.; Zhao, H.; Zhang, L.; Su, Y.; Lv, Y. BSA-Templated MnO<sub>2</sub> Nanoparticles as Both Peroxidase and Oxidase Mimics. *Analyst* **2012**, *137*, 4552–4558. [[CrossRef](#)] [[PubMed](#)]
17. Mu, J.; Zhang, L.; Zhao, M.; Wang, Y. Co<sub>3</sub>O<sub>4</sub> Nanoparticles as an Efficient Catalase Mimic: Properties, Mechanism and Its Electrocatalytic Sensing Application for Hydrogen Peroxide. *J. Mol. Catal. A Chem.* **2013**, *378*, 30–37. [[CrossRef](#)]
18. Qin, W.; Su, L.; Yang, C.; Ma, Y.; Zhang, H.; Chen, X. Colorimetric Detection of Sulfite in Foods by a TMB–O<sub>2</sub>–Co<sub>3</sub>O<sub>4</sub> Nanoparticles Detection System. *J. Agric. Food Chem.* **2014**, *62*, 5827–5834. [[CrossRef](#)] [[PubMed](#)]
19. Liao, H.; Liu, Y.; Chen, M.; Wang, M.; Yuan, H.; Hu, L. A Colorimetric Heparin Assay Based on the Inhibition of the Oxidase Mimicking Activity of Cerium Oxide Nanoparticles. *Microchim. Acta* **2019**, *186*, 1–6. [[CrossRef](#)] [[PubMed](#)]
20. Xia, X.; Zhang, J.; Lu, N.; Kim, M.J.; Ghale, K.; Xu, Y.; McKenzie, E.; Liu, J.; Ye, H. Pd–Ir Core–Shell Nanocubes: A Type of Highly Efficient and Versatile Peroxidase Mimic. *ACS Nano* **2015**, *9*, 9994–10004. [[CrossRef](#)]
21. Biswas, S.; Tripathi, P.; Kumar, N.; Nara, S. Gold Nanorods as Peroxidase Mimetics and Its Application for Colorimetric Biosensing of Malathion. *Sens. Actuators B Chem.* **2016**, *231*, 584–592. [[CrossRef](#)]
22. Ma, Y.; Zhang, Z.; Ren, C.; Liu, G.; Chen, X. A Novel Colorimetric Determination of Reduced Glutathione in A549 Cells Based on Fe<sub>3</sub>O<sub>4</sub> Magnetic Nanoparticles as Peroxidase Mimetics. *Analyst* **2012**, *137*, 485–489. [[CrossRef](#)]
23. Park, J.Y.; Jeong, H.Y.; Kim, M.I.; Park, T.J. Colorimetric Detection System for Salmonella Typhimurium Based on Peroxidase-like Activity of Magnetic Nanoparticles with DNA Aptamers. *J. Nanomater.* **2015**, *2015*, 527126. [[CrossRef](#)]
24. Ren, H.; Ma, T.; Zhao, J.; Zhou, R. Vc-Functionalized Fe<sub>3</sub>O<sub>4</sub> Nanocomposites as Peroxidase-like Mimetics for H<sub>2</sub>O<sub>2</sub> and Glucose Sensing. *Chem. Res. Chin. Univ.* **2018**, *34*, 260–268. [[CrossRef](#)]
25. Kong, Q.; Wang, Y.; Zhang, L.; Ge, S.; Yu, J. A Novel Microfluidic Paper-Based Colorimetric Sensor Based on Molecularly Imprinted Polymer Membranes for Highly Selective and Sensitive Detection of Bisphenol A. *Sens. Actuators B Chem.* **2017**, *243*, 130–136. [[CrossRef](#)]
26. Fan, C.; Liu, J.; Zhao, H.; Li, L.; Liu, M.; Gao, J.; Ma, L. Molecular Imprinting on PtPd Nanoflowers for Selective Recognition and Determination of Hydrogen Peroxide and Glucose. *RSC Adv.* **2019**, *9*, 33678–33683. [[CrossRef](#)]
27. Guo, L.; Zheng, H.; Zhang, C.; Qu, L.; Yu, L. A Novel Molecularly Imprinted Sensor Based on PtCu Bimetallic Nanoparticle Deposited on PSS Functionalized Graphene with Peroxidase-like Activity for Selective Determination of Puerarin. *Talanta* **2020**, *210*, 120621. [[CrossRef](#)] [[PubMed](#)]
28. Cao, Y.; Huang, Z.; Luo, L.; Li, J.; Li, P.; Liu, X. Rapid and Selective Extraction of Norfloxacin from Milk Using Magnetic Molecular Imprinting Polymers Nanoparticles. *Food Chem.* **2021**, *353*, 129464. [[CrossRef](#)] [[PubMed](#)]
29. Gao, L.; Zhuang, J.; Nie, L.; Zhang, J.; Zhang, Y.; Gu, N.; Wang, T.; Feng, J.; Yang, D.; Perrett, S. Intrinsic Peroxidase-like Activity of Ferromagnetic Nanoparticles. *Nat. Nanotechnol.* **2007**, *2*, 577–583. [[CrossRef](#)] [[PubMed](#)]
30. Li, Q.; Tang, G.; Xiong, X.; Cao, Y.; Chen, L.; Xu, F.; Tan, H. Carbon Coated Magnetite Nanoparticles with Improved Water-Dispersion and Peroxidase-like Activity for Colorimetric Sensing of Glucose. *Sens. Actuators B Chem.* **2015**, *215*, 86–92. [[CrossRef](#)]
31. Wang, J.; Yang, X.; Wei, T.; Bao, J.; Zhu, Q.; Dai, Z. Fe-Porphyrin-Based Covalent Organic Framework as a Novel Peroxidase Mimic for a One-Pot Glucose Colorimetric Assay. *ACS Appl. Bio Mater.* **2018**, *1*, 382–388. [[CrossRef](#)] [[PubMed](#)]
32. Wang, J.; Huang, F.; Wang, X.; Wan, Y.; Xue, Y.; Cai, N.; Chen, W.; Yu, F. Hierarchically Structured Fe<sub>3</sub>O<sub>4</sub>-Doped MnO<sub>2</sub> Microspheres as an Enhanced Peroxidase-like Catalyst for Low Limit of Detection. *Process Biochem.* **2019**, *83*, 35–43. [[CrossRef](#)]
33. Peng, F.F.; Zhang, Y.; Gu, N. Size-Dependent Peroxidase-like Catalytic Activity of Fe<sub>3</sub>O<sub>4</sub> Nanoparticles. *Chinese Chem. Lett.* **2008**, *19*, 730–733. [[CrossRef](#)]
34. Xiong, Y.H.; Chen, S.H.; Ye, F.G.; Su, L.J.; Shen, S.F.; Zhao, S.L. Preparation of magnetic core–shell nanoflower Fe<sub>3</sub>O<sub>4</sub>@MnO<sub>2</sub> as reusable oxidase mimetics for colorimetric detection of phenol. *Anal. Methods* **2014**, *7*, 1300–1306. [[CrossRef](#)]
35. Lian, J.J.; Liu, P.; Li, X.C.; Gao, L.N.; Luo, X.L.; Zhang, X.; Shi, Z.Q.; Liu, Q.Y. Perylene diimide-modified magnetic  $\gamma$ -Fe<sub>2</sub>O<sub>3</sub>/CeO<sub>2</sub> nanoparticles as peroxidase mimics for highly sensitive colorimetric detection of Vitamin C. *Appl. Organomet. Chem.* **2019**, *33*, e4884. [[CrossRef](#)]
36. Mendes, C.; Buttchevitz, A.; Kruger, J.H.; Bernardl, L.S.; Oliveira, P.R.; Silva, M. Quantitative analysis of norfloxacin in beta-Cyclodextrin inclusion complexes-development and validation of a stability-indicating HPLC method. *Anal. Sci.* **2015**, *31*, 1083–1089. [[CrossRef](#)]
37. Kowalski, C.; Roliński, Z.; Sawik, T.; Gód, B.K.; Roliń, Z. determination of norfloxacin in chicken tissues by HPLC with fluorescence detection determination of norfloxacin in chicken tissues by HPLC with fluorescence detection. *Liq. Chromatogr. R. T.* **2005**, *28*, 121–135. [[CrossRef](#)]
38. Cui, J.L.; Zhang, K.; Huang, Q.X.; Yu, Y.Y.; Peng, X.Z. An indirect competitive enzyme-linked immunosorbent assay for determination of norfloxacin in waters using a specific polyclonal antibody. *Anal. Chim. Acta.* **2011**, *688*, 84–89. [[CrossRef](#)] [[PubMed](#)]
39. Chen, S.; Su, X.; Yuan, C.; Jia, C.Q.; Yang, Y. A magnetic phosphorescence molecularly imprinted polymers probe based on manganese-doped ZnS quantum dots for rapid detection of trace norfloxacin residual in food. *Spectroch. Acta. A.* **2021**, *253*, 119577. [[CrossRef](#)]
40. Rodríguez-Díaz, R.C.; Aguilar-Caballós, M.P.; Gómez-Hens, A. Sensitive Determination of Fluoroquinolone Antibiotics in Milk Samples Using Time-Resolved Methodology. *Anal. Lett.* **2004**, *37*, 1163–1175. [[CrossRef](#)]

41. Qiu, X.Q.; Gu, J.; Yang, T.Q.; Ma, C.Q.; Li, L.; Wu, Y.M.; Zhu, C.; Gao, H.; Yang, Z.C.; Wang, Z.R.; et al. Sensitive determination of Norfloxacin in milk based on beta-cyclodextrin functionalized silver nanoparticles SERS substrate. *Spectrochim. Acta A Mol. Biomol. Spectrosc.* **2022**, *276*, 121212. [[CrossRef](#)]
42. Xie, Y.; Zheng, Y.; Shui, H.Z.; Wu, Z.J.; Yu, X.H.; Zhang, C.G.; Feng, S. Preparation of molecularly imprinted polymers based on covalent organic frameworks and their application to selective recognition of trace norfloxacin in milk. *Chin. J. Chromatogr.* **2022**, *40*, 1–9. [[CrossRef](#)] [[PubMed](#)]

**Disclaimer/Publisher's Note:** The statements, opinions and data contained in all publications are solely those of the individual author(s) and contributor(s) and not of MDPI and/or the editor(s). MDPI and/or the editor(s) disclaim responsibility for any injury to people or property resulting from any ideas, methods, instructions or products referred to in the content.